JOURNAL OF MAGNETIC RESONANCE, Series A 102, 116–121 (1993)

COMMUNICATIONS

A Three-Dimensional Method for the Separation of Zero-Quantum Coherence and NOE in NOESY Spectra

HONG WANG,* † GARY D. GLICK,† AND ERIK R. P. ZUIDERWEG* ‡

* *Biophysics Research Division and † Department of Chemistry, The University of Michigan, Ann Arbor, Michigan 48109*

Received November 25, 1992; revised January 5, 1993

Cross-peak intensities in a two-dimensional nuclear Overhauser enhancement spectrum are related to the proximity of the protons whose shifts are correlated by the experiment (*1*). The cross-peak intensities yield quantitative distance data when analyzed by full-relaxation-matrix methods (*2–4*); alternatively quantitative distance information is obtained from the buildup rate of the NOE cross peaks extrapolated to the limit of zero NOE mixing time (*5*). Both approaches have their advantages and limitations and can be expected to coexist.

The NOE buildup rate approach has as advantages that a selection of cross peaks can be analyzed and that the computational methods are simple and fast. However, the requirement that the data be measured at very short NOE mixing times causes technical problems: zero-quantum coherence (ZQC) transfer interferes with the proper analysis of NOE cross peaks between scalar-coupled resonances (*5*). This problem is particularly troublesome in the analysis of NOESY spectra of small oligonucleotides because of the important role of NOEs between scalar-coupled nuclei for conformational determination of these molecules (*6*) and because of relatively slow transverse relaxation of the ZQC.

The problem of ZQC transfer was originally approached by using a random variation (jittering) of the length of the NOE mixing time or of the placement of a π pulse in the mixing time from t_1 increment to t_1 increment (*5*). Since the mixing-time dependence of ZQC is oscillatory, (Fourier) transformation of t_1 will lead to a spread of the ZQC cross peak along F_1. In unfavorable cases, this spread intensity becomes the dominating t_1 noise in the spectrum and limits data analysis. An example of the noise caused by the jittering approach is shown in Fig. 1. A related alternative approach is to coadd several to tens of different NOE spectra recorded with slightly different mixing times (*7*). When the mixing times are judiciously chosen, efficient suppression of the ZQC can be achieved "in place." With this method the creation of additional noise is avoided but one is never quite sure if complete cancellation has occurred since a range of frequencies needs to be considered even for a single cross peak (vide infra). The third approach is to vary the mixing time—or the placement of a π pulse in the mixing time—proportionally to the evolution time (*8*). Upon (Fourier) transformation, the ZQC peaks are shifted away from the NOESY cross peaks and the diagonal. A total of at least four ZQC cross peaks will show in the spectrum for every scalar correlation (at frequencies $\pm\kappa\Delta\Omega$ around the diagonal and cross peaks, with κ the ratio of the increment in t_1 and mixing time and $\Delta\Omega$ the ZQC frequencies). The ZQC peaks are in double-antiphase dispersion when the NOE peaks are phased to absorption. Because of the proliferation and unfavorable shape of the shifted ZQC peaks, other coincidental overlaps can be unintentionally generated in this approach.

The problem associated with all of the above methods is that the ZQC peaks stay in the two-dimensional NOESY plane, either smeared out, (partially) averaged out, shifted out, or a combination of these. Here, we propose placing the ZQC-transfer peaks into a third dimension orthogonal to the NOESY plane, thereby minimizing interference between the NOE and ZQC peaks. The experiment is carried out by acquiring two-dimensional NOE spectra as a function of a linear incrementation of the mixing time—or the placement of a π pulse in the mixing time. The three-dimensional sequence used is

$$\mathrm{RD}\text{–}\pi/2\text{–}t_1\text{–}\pi/2\text{–}(\tau_m - t_2)/2\text{–}\pi\text{–}(\tau_m + t_2)/2\text{–}\pi/2\text{–}t_3.$$

With a phase cycle to suppress transfer of the non-zero-quantum-coherence orders and quadrature detection in t_1 and t_3, one obtains the modulations for an AX spin system

$$\exp(i\Omega_A t_1)\sin(\pi J_{AX} t_1) \times \cos[(\Omega_A - \Omega_X)t_2]\exp(i\Omega_X t_3)\sin(\pi J_{AX} t_3)$$

and

$$\exp(i\Omega_A t_1)\cos(\pi J_{AX} t_1)\exp(i\Omega_X t_3)\cos(\pi J_{AX} t_3)$$

‡ To whom correspondence should be addressed.

1064-1858/93 $5.00

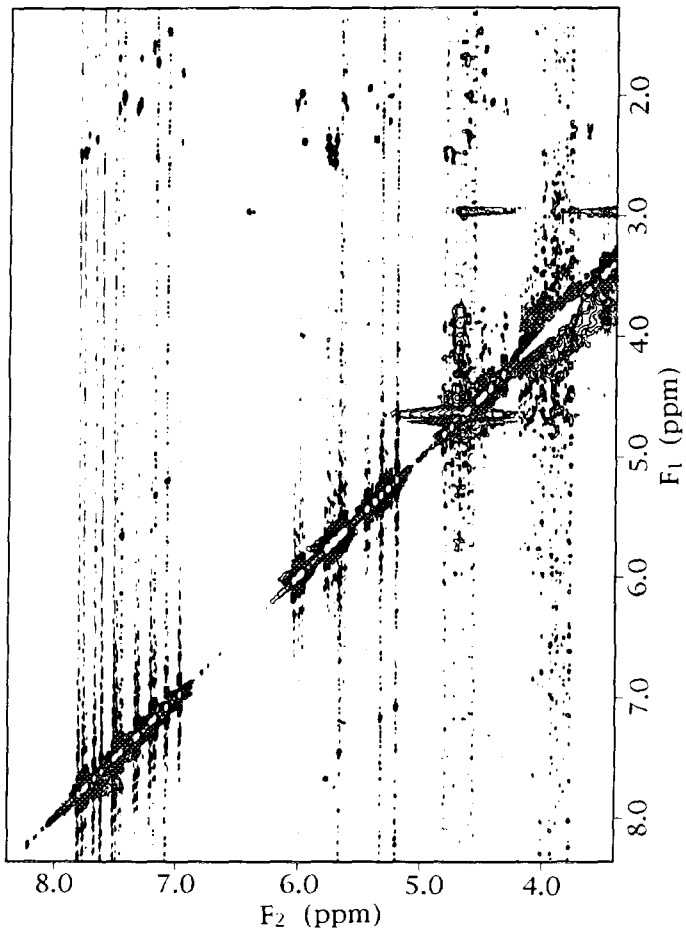

FIG. 1. NOESY spectrum (τ_m = 25 ms) of a 2 m*M* solution of cross-linked DNA hairpin *d*(TGCGAATTCGCT) (*13*) in ^2H_2O, 50 m*M* NaCl, 10 m*M* phosphate, p^{2}H 7.0, *T* = 12°C, recorded on a Bruker AMX500 spectrometer. Five hundred twelve TPPI t_1 increments of 2048 points each were collected. For each increment, 8 scans were taken at six random NOE mixing times with variation of 10% around 25 ms and coadded (48 scans per t_1 increment). An (x, y, $-x$, $-y$) phase cycle of the last $\pi/2$ pulse and receiver was used to suppress non-zero-quantum coherences; axial peaks were suppressed by inversion of the first pulse and receiver phases. Recycling delay was six seconds. The spectrum was processed with 1 Hz line broadening in F_2 and a 90°-shifted squared-sine-bell window function in F_1. Positive and negative peaks are plotted. Some baseline artifacts caused by strong contaminant signals are seen; the upfield part of the spectrum is not shown for these reasons as well.

for ZQC and NOE correlations between the scalar- and dipolar-coupled resonances at frequencies Ω_A and Ω_X, respectively. After three-dimensional Fourier transformation one obtains in-phase absorptive NOE cross peaks in the (F_1, F_3) plane at F_2 = 0 ("axial" or "NOE" plane) and ZQC peaks in (F_1, F_3) plane(s) at frequency(s) | $\Omega_A - \Omega_X$ | in F_2. The ZQC peaks are in antiphase dispersion mode in F_1 and F_3 but absorptive mode in F_2.

Figure 2 shows the NOE plane of the three-dimensional experiment. The data were obtained in the same experimental time, with the same resolution, and with the same total number of scans as the two-dimensional spectrum shown in Fig. 1. It is immediately obvious that the quality of the NOE data has improved dramatically by placing the ZQC interference in the third dimension; the noise streaks have disappeared. For instance, NOE cross peaks between deoxyribose H3′ (F_1 = 4.6 ppm) and H4′ (F_3 = 4 ppm) can easily be discerned in the 3D data, while noise hides those peaks in the 2D data (Fig. 1). The quality improvement is further illustrated by comparing stacked plots of the 2D spectrum and the NOE plane of the 3D data in the cytosine H5–H6 region (Fig. 3). The buildup rates of these cross peaks are often used as internal distance rulers for NOE calibration. It is evident that these intensities can be obtained with much

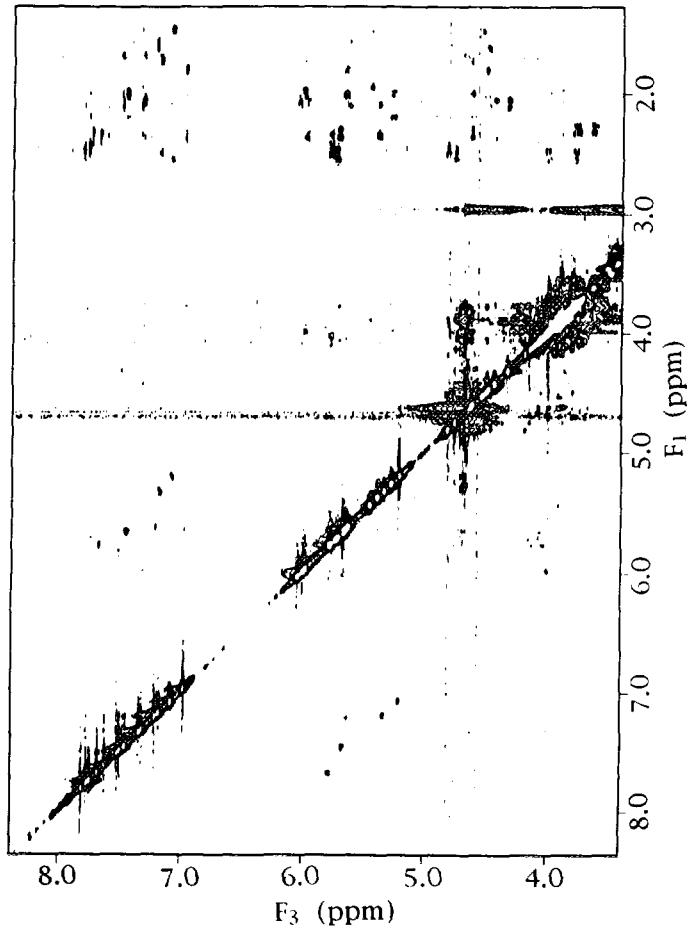

FIG. 2. Axial or NOE plane from the three-dimensional clean NOESY experiment (τ_m = 25 ms) of *d*(TGCGAATTCGCT) recorded with the pulse sequence RD–$\pi/2$–t_1–$\pi/2$–($\tau_m - t_2$)/2–π–($\tau_m + t_2$)/2–$\pi/2$–t_3. An (x, y, $-x$, $-y$) phase cycling of the last $\pi/2$ pulse and receiver was used to suppress non-zero-quantum coherences. Axial peaks were not suppressed. TPPI phase incrementation was used in t_1; no quadrature was used in t_2. Five hundred twelve t_1 increments of four scans each (2048 t_3 points) were recorded for every of the 12 t_2 incrementations of 250 μs (a ZQC spectral width of 2000 Hz). The 3D matrix was processed the same way in F_1 and F_3 as the 2D experiment using Felix 2.05 (Hare Research, Inc). The t_2 data were extended to 32 real points using mirror-image linear prediction (*14*), multiplied by a 90°-shifted sine bell, zero filled to 64 points, and subjected to real Fourier transformation. The final real matrix was 512 × 32 × 2048 points (F_1, F_2, F_3).

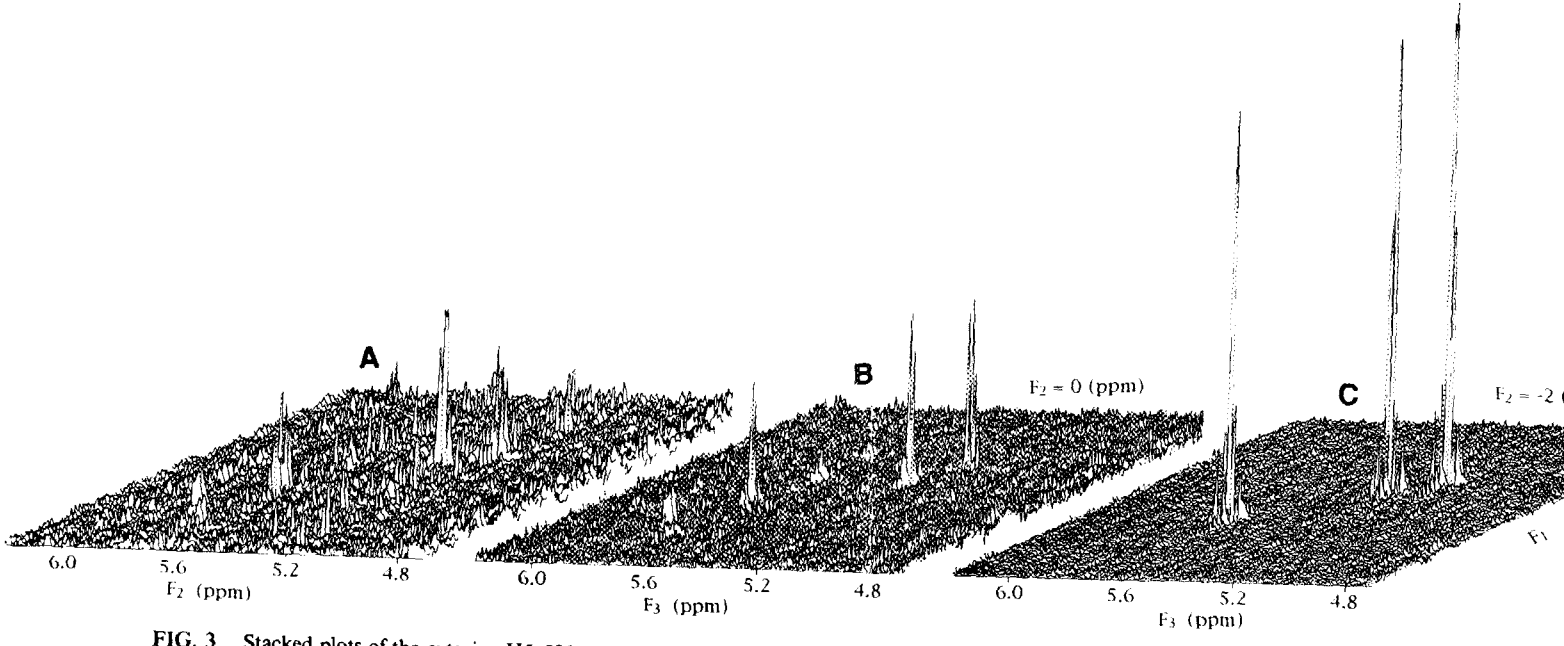

FIG. 3. Stacked plots of the cytosine H5–H6 cross-peak regions of the 2D spectrum (A); the NOE plane of the 3D spectrum (B); and (C) the ZQC plane for these cross peaks in the 3D spectrum ($F_2 = -2.0$ ppm). The vertical scale is the same in the three panels.

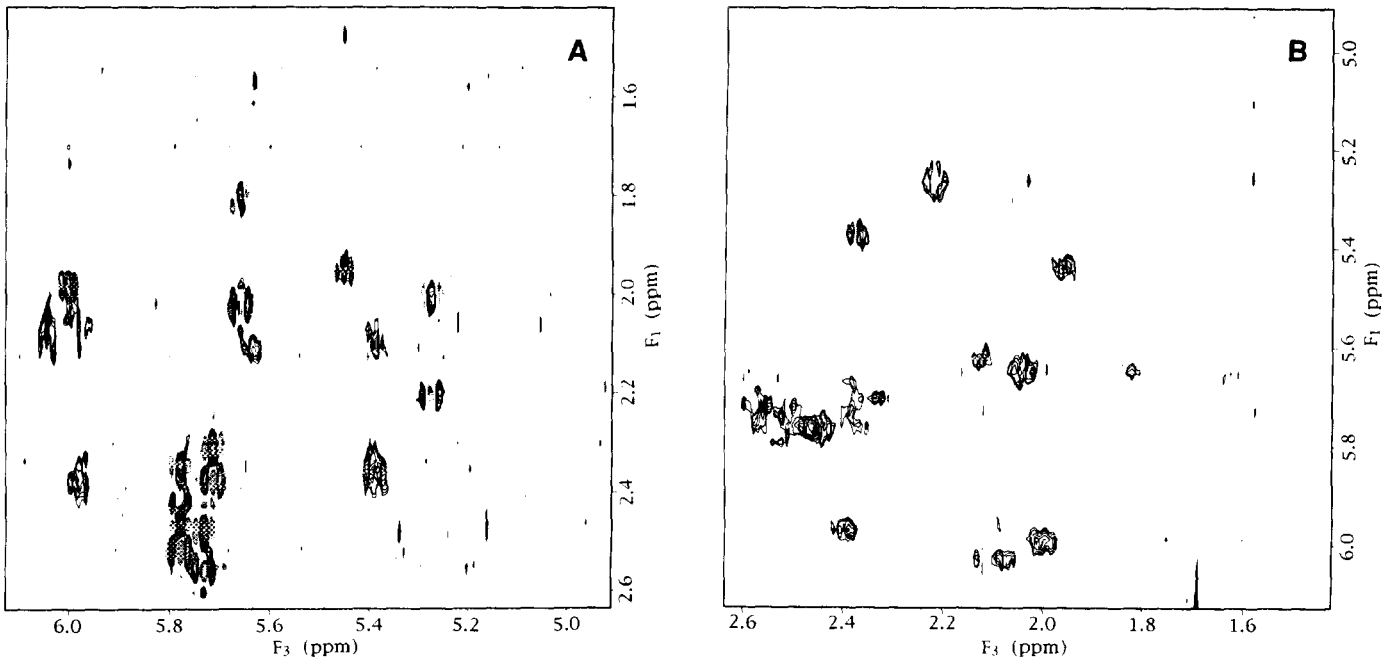

FIG. 4. Expanded regions of the NOESY plane of the 3D spectrum in Fig 2. (A) The 2′/2″(F_1)–1′(F_3) area; (B) the 1′(F_1)–2′/2″(F_3) area. Negative intensities are plotted with dashed contour lines.

higher precision from the 3D data than from the noise-ridden two-dimensional spectrum.

Since the total acquisition time and number of scans are equal for the two-dimensional and three-dimensional data, and since no additional (incrementable) delays are introduced in the 3D experiment, one expects the sensitivity of the NOE plane of the 3D experiment to be equal to that of the full 2D experiment. Comparison of the stacked plots (Fig. 3) shows that a slight reduction in the sensitivity of the 3D data occurred. This is caused by the windowing functions that were used prior to the Fourier transformation $t_2 \rightarrow F_2$, leading to a NOE cross peak that has finite linewidth in the F_2 dimension and thus reduced intensity at $F_2 = 0$. Windowing can potentially be avoided when linear prediction or MEM parametrization (9) at $F_2 = 0$ is used instead of linear prediction followed by Fourier transformation as was carried out here.

Figure 3C, taken from the 3D spectrum at a frequency $F_2 = -2.0$ ppm, shows the ZQC peaks associated with the three cytosine H5–H6 correlations. Since the ZQC peaks are large compared to the NOE peaks, one concludes that it is very desirable to place these large ZQC peaks into a third dimension rather than accept them in one form or another in a two-dimensional NOESY spectrum.

Even in the three-dimensional spectrum the NOESY plane is not completely devoid of coherence transfers. The strongest occurrence of these interferences, evidenced by negative dispersive components, is in the 2′/2″–1′ region (F_1, F_3) as is shown in Fig. 4A. The jittered 2D data have the same deficiencies in this area (Fig 1; enlargement not shown). In contrast, cross peaks in the symmetrically related 1′–2′/2″ region are in absorption (Fig. 4B). Figure 5A shows an F_2 cross section perpendicular to the NOE plane at (F_1, F_3) coordinates of a 2′/2″–1′ cross peak in the area of Fig. 4A. The NOE intensity is found at 0 ppm and is very small for this proton pair (the prochirally related NOE is much larger). Two ZQC frequencies are observed; in addition to the ZQC

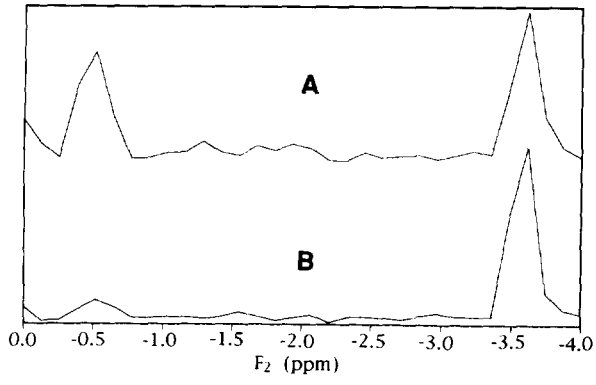

FIG. 5. Cross sections through the 3D clean NOESY spectrum parallel to F_2. (A) Cross section taken at the (F_1, F_3) coordinates of one of the H2′ (1.48 ppm)–H1′ (5.45 ppm) cross peaks (see Fig. 4A). (B) Cross section taken at the (F_1, F_3) coordinates of one of the H1′ (5.45 ppm)–H2′ (1.48 ppm) cross peaks (see Fig. 4B). The NOE intensity is found at 0 ppm and ZQCs at −0.5 and −3.5 ppm. The cross sections were obtained from a skyline projection of 10 × 20 cross sections around the mentioned (F_1, F_3) coordinates to capture all intensities.

corresponding to the difference in frequency between H1′ and H2′/H2″ ($\Delta\Omega$ = 3–4 ppm) one also observes a slow oscillation at the difference frequency $\Omega_{H2'}-\Omega_{H2''}$. When $\Omega_{H2'}-\Omega_{H2''}$ becomes small, this ZQC transfer can no longer be separated from NOE. In limiting cases, strong-coupling effects come into play (*10*), which make the 2′–2″ coherence behave as zz magnetization and hence not labelable or cancelable by frequency. The distortions in the NOESY plane are due to these low-frequency components. Figure 5B shows the symmetrically related F_2 cross section at coordinates of the related 1′–2′/2″ cross peak in the area of Fig. 4B. The low-frequency component is here strongly suppressed (vide infra); consequently the NOE plane is virtually undisturbed in this region.

Multiple ZQC pathways are possible in more complex spin systems like deoxyribose H2′–H2″–H1′. For a three-spin system, three coherence-transfer pathways involving ZQC give rise to interference in a NOESY spectrum. In the weak-coupling limit, the following pathways are relevant for the mutually coupled system I–S–Q, all starting on I and ending on S:

$$I_y[t_1 = 0] \xrightarrow{J_{IS}} 2I_xS_z[t_1 = t_1] \xrightarrow{90^\circ_x}$$

$$(I_xS_y - I_yS_x)[\tau_m = 0] \xrightarrow{J_{IQ},J_{SQ},\Omega_S,\Omega_I}$$

$$(I_xS_y - I_yS_x)\cos\pi(J_{IQ} - J_{SQ})$$

$$\times \tau_m\cos(\Omega_S - \Omega_I)\tau_m[\tau_m = \tau_m]$$

(Direct Path)

$$I_y[t_1 = 0] \xrightarrow{J_{IQ}} 2I_xQ_z[t_1 = t_1] \xrightarrow{90^\circ_x}$$

$$(I_xQ_y - I_yQ_x)[\tau_m = 0] \xrightarrow{J_{IS},J_{QS},\Omega_I,\Omega_Q}$$

$$(2I_xQ_xS_z + 2I_yQ_yS_z)\sin\pi(J_{IS} - J_{QS})$$

$$\times \tau_m\cos(\Omega_I - \Omega_Q)\tau_m[\tau_m = \tau_m]$$

(Associated Path)

$$I_y[t_1 = 0] \xrightarrow{J_{IQ},J_{IS}} 4I_yS_zQ_z[t_1 = t_1] \xrightarrow{90^\circ_x}$$

$$(2I_zS_xQ_x + 2I_zS_yQ_y)[\tau_m = 0] \xrightarrow{J_{IQ},J_{IS},\Omega_S,\Omega_Q}$$

$$(S_xQ_y - S_yQ_x)\sin\pi(J_{IS} - J_{IQ})$$

$$\times \tau_m\cos(\Omega_S - \Omega_Q)\tau_m[\tau_m = \tau_m]$$

(Remote Path)

The read pulse converts all three terms to observable magnetization with an F_3 frequency of S. In the 3D spectrum, we thus expect to find three ZQC-mediated cross peaks for the single NOE cross peak between I and S: (Ω_I, $\Omega_I - \Omega_S$, Ω_S), (Ω_I, $\Omega_I - \Omega_Q$, Ω_S), and (Ω_I, $\Omega_Q - \Omega_S$, Ω_S) for the direct, associated, and remote peaks in F_1, F_2, F_3, respectively. The relative intensities of these ZQC terms depend on the sizes and signs of the scalar couplings and the durations of t_1 and τ_m. In the 2′/2″–1′ region, I, Q, and S correspond to 2′, 2″, and 1′, respectively. For DNA, the expected scalar couplings are $J_{1'-2'}$ (J_{IS}) = 8 Hz, $J_{1'-2''}$ (J_{SQ}) = 5 Hz, and $J_{2'-2''}$ (J_{IQ}) = −14 Hz (*11, 12*). With τ_m = 25 ms, the direct path is almost completely suppressed in this area [$\cos\pi(J_{1'-2''} - J_{2'-2''})\tau_m = 0$], the remote path is fully active [$\sin\pi(J_{1'-2'} - J_{2'-2''})\tau_m = 1$], and the associated path is partially active [$\sin\pi(J_{1'-2''} - J_{1'-2'})\tau_m = 0.2$]. This explains why only two frequencies are seen in Fig. 5. The intensity of the low-frequency-associated ZQC is enhanced with respect to that of the high-frequency remote ZQC because of the integral of the transfer function during t_1. The fast remote ZQC resonates at −3.5 ppm, different as expected from the −4.0 ppm direct ZQC, derived from the difference in chemical shift between the protons correlated in the cross peak (see legend to Fig. 5).

For the symmetrically related cross peaks, the low-frequency component is the remote peak and the high-frequency component is the associated peak. The relative intensities are different here; the low-frequency peak is suppressed (see Figs. 4B and 5B) because of a small integral (0.1) of the transfer function during t_1. As a result, the NOE cross peaks are virtually unperturbed and thus best studied in this region.

In summary, we have demonstrated that ZQC interference in NOESY spectra can be substantially reduced by recording the spectrum in a three-dimensional mode. In analogy to the nomenclature originating from coherence/dipolar conflicts in TOCSY/ROESY, we call our experiment 3D clean NOESY. The approach generates high-quality data devoid of interfering noise and ZQC overlap of NOESY peaks, allowing more reliable analysis of NOEs between scalar-coupled protons. This improvement should ultimately result in better defined NMR-derived three-dimensional structures. The approach also visualizes many coherence-transfer pathways that potentially can be used for spin system delineation and coupling constant estimation. A potential drawback of the method is that relatively large amounts of disk space are required for the acquisition of the data.

ACKNOWLEDGMENTS

This research was carried out partially under support of NSF (Grant MCB9218573) to E.R.P.Z. G.D.G. thanks NIH (Grant GM 46831) for partial support of this work. The 500 MHz NMR spectrometer (Chemistry Department) was funded in part through the NIH Shared Instrumentation Program (Grant RR 06739). We thank Dr. D. R. Hare (Hare Research, Inc.) for making Felix 2.05 available.

REFERENCES

1. S. Macura, Y. Huang, D. Suter, and R. R. Ernst, *J. Magn. Reson.* **43**, 258 (1981).

2. E. T. Olejniczak, R. T. Gampe, Jr., and S. W. Fesik, *J. Magn. Reson.* **67,** 28 (1986).
3. R. Boelens, T. M. G. Koning, G. A. Van der Marel, J. H. van Boom, and R. Kaptein, *J. Magn. Reson.* **82,** 290 (1989).
4. B. A. Borgias, M. Gochin, D. J. Kerwood, and T. J. James, *Prog. NMR Spectrosc.* **22,** 83 (1990).
5. S. Macura, K. Wüthrich, and R. R. Ernst, *J. Magn. Reson.* **47,** 351 (1982).
6. S-G. Kim, L-J. Lin, and B. R. Reid, *Biochemistry* **31,** 3564 (1992).
7. M. Rance, G. Bodenhausen, G. Wagner, K. Wüthrich, and R. R. Ernst, *J. Magn. Reson.* **62,** 497 (1985).
8. S. Macura, K. Wüthrich, and R. R. Ernst, *J. Magn. Reson.* **43,** 269 (1982).
9. D. S. Stephenson, *Prog. NMR Spectrosc.* **20,** 515 (1988).
10. L. E. Kay, J. N. Scarsdale, D. R. Hare, and J. H. Prestegard, *J. Magn. Reson.* **68,** 515 (1984).
11. K. Weiz, R. H. Shafer, W. Egan, and T. L. James, *Biochemistry* **32,** 7477 (1992).
12. H. Widmer and K. Wüthrich, *J. Magn. Reson.* **74,** 316 (1987).
13. G. D. Glick, S. E. Osborne, D. S. Knitt, and J. P. Marino, Jr., *J. Am. Chem. Soc.* **114,** 5447 (1992).
14. G. Zhu and A. Bax, *J. Magn. Reson.* **90,** 405 (1990).